Chapter 8

Transmembrane transport via integral proteins

8-1. Introduction: Passive carrier-mediated transmembrane transport

Black lipid membranes, phospholipid bilayers containing no protein, are virtually impermeable to hydrophilic solutes, even water itself. The generality is that all hydrophilic solutes require the presence of some special transmembrane molecule, usually a protein, to traverse the bilayer. Some integral membrane proteins serve simply as conduits for specific solutes. For example, an integral transmembrane protein aquaporin transports water selectively, passively (Agre, 1993), and a potassium-selective channel protein serves the time-independent I_K current (Winslow et al., 1999) whose conductances seem purely passive, independent of concentration, but dependent on transmembrane voltage. They are highly selective, though imperfect!

The ionic channels with time- and voltage-dependent kinetics discussed in Chapter 7 are passive, even while being selective: the currents are driven solely by the electrochemical gradients for the ion. Such channels are not energetically coupled, and when open they allow the passage of many ions, often thousands per millisecond. Their selectivity is not by any means total, but is limited to a few similarly charged and sized ions or ionized solutes. These are not usually classed as “transporters”, but rather as channels, because when they are open the rate of transfer depends on the driving forces across the membrane and not on the rate of change of conformational state of the protein. In contrast, carriers or transporters selectively bind substrates at a surface site and carry the substrate across the membrane at a rate depending on the state of the carrier rather than on the driving force for substrate. Thus the transporter-facilitated flux for substrate depends on the number of carrier proteins per unit surface area of membrane, the fraction of sites filled, and the rate of comformational state to carry the active site from one side of the membrane to the other.

How does one distinguish carrier-mediated transport from that due to channels or other passive leaks? The somewhat vague rule is that when a solute traverses the membrane faster than “expected”, it is likely that a transporter molecule can be found to explain the flux. The

"expected" permeability is that estimated by comparison with other molecules of similar water/lipid solubility ratios and molecular size and hydrophobicity (Tanford, 1961; Stein, 1986). This does not distinguish a facilitating transporter from a channel such a as voltage-dependent ionic channel.The key difference is that a transporter is "saturable": the flux of solute transported reaches a maximum at high substrate concentrations.

8-1.1. Evidence for permeation by facilitating transporters

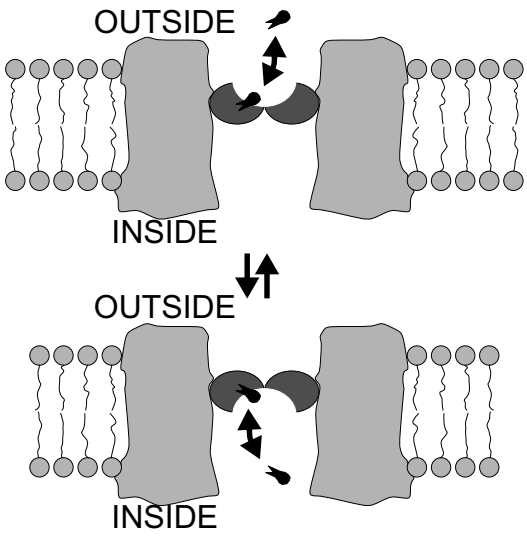

Figure 8-1: Facilitated transport. After a membrane transporter binds a solute, there is a conformational change to flip the site (and the bound solute) to face the opposite side of the membrane, allowing release of the solute on the other side of the membrane.

By facilitated transport, as mediated through substrate binding and a conformational state change as in Fig. 8-1, one means that the transport of a substrate across the membrane is faster than it would be without the presence of the transporter protein. The transport occurs without coupling to ATP and without the need for energy supplied by another solute moving down its electrochemical gradient. A requirement for energy supplied by ATP is termed "active transport". The requirement for coupling to the dissipation of an energy potential for *another* solute is termed "coupled transport"; an example of facilitated exchange is the sodium-calcium exchanger: it uses the sodium electro-chemical potential exchanging 3 sodium ions moving down their potential gradient into the cell to drive one calcium ion outward, or vice versa. Passive facilitated transport was termed 'facilitated diffusion' when it was first identified and characterized. This early era is reviewed in the pioneering studies of Wilbrandt and Rosenberg (1961) and the texts by W.D. Stein (1967, 1986).

One should suspect facilitation of flux via a special transporter when:

1. Transmembrane flux rises to a maximum plateau as substrate concentration is raised, rather than following Fick's first law. In other words, the apparent conductivity diminishes with increasing concentration. This is "*saturation kinetics*", and is a strong inference, although it is dependent on parallel evidence in the experiment that the fluxes of other unrelated solutes are unchanged by the concentrations of the particular substrate.

2. Transport of a solute is reduced in the presence of specific molecules of analogous structure. This is *competition,* and is also a strong inference.
3. There is inhibition of tracer-labeled substrate transfer by the presence of non-tracer mother substrate (that is, *self-competition* by the unlabeled substrate). This observation is almost sure evidence.
4. There is facilitation of the unidirectional tracer-labeled substrate flux by the flux of a molecule of similar structure down its electrochemical gradient in the opposite direction. This is a special case, *exchange transport facilitation*, that virtually guarantees the existence of a transporter.
5. There is inhibition of flux by unlike substances but which are specific to the transport of specific permeant. These *transport blockers*, like enzyme blockers, are usually poisons which bind tightly to the transporter and stop its action. (These inhibitors fall into the classes of competitive inhibitors, ones that can be displaced from the active site by high substrate concentrations, and non-competitive inhibitors, ones which bind elsewhere on the transporter molecule but induce conformational changes that preclude or reduce substrate binding to the transporter or the conformational change effecting the translocation across the membrane.) The inhibition must be specific, not affecting the membrane itself or the fluxes of unrelated solutes.
6. *There are inexplicably high fluxes*, higher than expected from the physicochemical characteristics of the substrate. This is not a very strongly inferential point, but does illustrate why transporters exist for so many solutes: normal rates of penetration are too slow to maintain the metabolic needs of the cell. No one had thought much about why the water permeability of cell membranes was so high, despite knowing that lipid bilayers were almost impermeable, until Peter Agre (1991) revealed the existence of an integral protein forming the aquaporin channel.

8-1.2. Unidirectional versus net fluxes.

The basis of the tracer method: Flux of a solute across a membrane is bidirectional. One can obtain a measure of the unidirectional flux in the mixing chamber experiment diagrammed in Fig. 8-2 by starting with a known concentration on side 1, a zero concentration on side 2 and then measuring the rates of change in concentrations on both sides. At very early times when $C_2 << C_1$ the net flux across the membrane equals the unidirectional flux since the return flux from side 2 to side 1 is negligible, so that Eq. 8-1 is a good approximation. The dependence of the rate on the concentration is expressed by the form of $k(C_1)$:

$$V_2 \frac{dC_2}{dt} = -k(C_1) \cdot C_1 \cdot V_1 \qquad (8\text{-}1)$$

However it is often more efficient to use tracers to measure the unidirectional fluxes for example when there is no chemical gradient across the membrane. Then by putting tracer into mixing chamber 1, and with zero tracer initially on side 2, the rate of tracer flux indicates the unidirectional flux for the mother substance under the existent conditions, i.e. the tracer flux provides the estimate of $k(C)$ at the ambient levels of C. This is important because when transport is carrier-mediated the tracer flux is controlled by the sum of the concentrations of the tracer, C^*, and the mother substance:

$$V_2 \frac{dC_2^*}{dt} = -k((C_1 + C_1^*) \cdot C_1^* \cdot V_1. \quad (8\text{-}2)$$

However by the definition that a tracer molecule is chemically identical to the mother solute molecule, and that the tracer concentration is many orders of magnitude smaller than that of the mother solute and therefore has negligible influence itself on the k(C), this equation reduces to:

$$V_2 \frac{dC_2^*}{dt} = -k(C_1) \cdot C_1^* \cdot V_1 \quad . \quad (8\text{-}3)$$

Since $k(C_1)$ is a constant that is not changed by changes in tracer concentration, the system is linear and first order so far as tracer flux is concerned.

This generality holds true even when many solutes affect the rate constant, so that by changing the concentrations of each of the influencing chemicals in a series of tracer flux measurements one can distinguish the varied effects, inhibitions, enhancements, competition, etc., exploring the variant conditions:

$$\frac{dC_2^*}{dt} = -k(C_1, C_2, A_1, ...Z_1, Z_2) \bullet C_1^* \quad , \quad (8\text{-}4)$$

where the subscripted C's, A's to Z's are the concentrations of all the various solutes interacting with the transporter. This expression holds true in this simple form only when all the C's are in steady state. In this state k(C, etc.) remains a constant and the tracer system equations are first order.

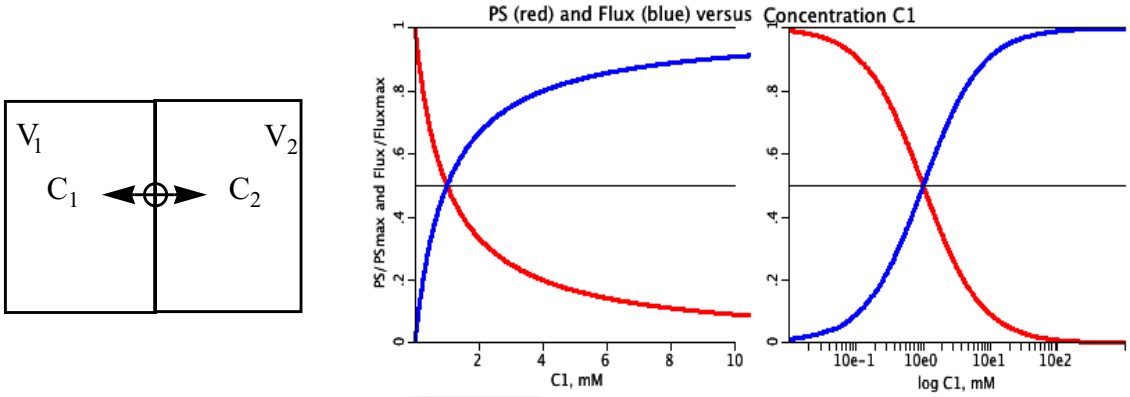

Figure 8-2: Two chambers with transmembrane flux via a facilitating transporter. *Left panel*: Two stirred tanks. The circle on the membrane represents the transporter, an integral protein. *Middle and right panels:* With $C_2 = 0$, and held there, one can measure the effective PS/PSmax (red lines) and the tracer flux/Fluxmax (blue lines) on linear and log plots as a function of non-tracer mother solute concentration, C_1. The flux is half maximal at $C_1 = K_m$; K_m is the equilibrium dissociation constant for substrate binding to the transporter, 1 mM in this case.

Unidirectional fluxes: These are measurable under two sets of conditions: (1) from tracer measurements when there is a source of tracer on one side of the membrane only, and (2) from measurements of non-tracer mother substrate when there is initially no substrate on the other side of the membrane. The advantage of using tracer methods is that one can get a measure of unidirectional flux even when there is mother substance on both sides, and one can therefore explore a wide variety of conditions. By Fick's first law the net exchange of substrate is

$$J_{S_{1,2}} = PC_1 - PC_2 , \tag{8-5}$$

where J_S is the net flux per unit area of membrane, mol s^{-1} cm^{-2}, P is permeability, cm s^{-1}, and C_1 and C_2 are the concentrations, mmol cm^{-3}, on the cis (side 1) and trans (side 2) sides of the membrane. The net flux is the difference between the two unidirectional fluxes PC_1 and PC_2.To measure the unidirectional flux, PC1, either C_2 must be 0 so one measure the rate of entry of substrate C into V2, or use tracer techniques. For "initial velocity studies",: the tracer or the mother substrate, is placed on side 1 and the concentrations on side 2 are obtained at a succession of times. At early times the concentration on side 2 is so low that the backflux, P times C_2, is negligible; the slope, dC_2/dt, can be determined as a best straight line for some time before the influence of the backflux diminishes the slope.

The strategy of examining the initial velocities before C_2 rises works well for studies of transporter fluxes. The initial slopes, as are found in a sequence of experiments at different mother substance concentrations, Fig. 8-3, upper, and the pseudo-steady state slopes plotted versus $C_1(t = 0)$, as in the lower panel. The result, Fig. 8-3 lower, is that the flux -to-substrate concentration relationship fits the relationship:

$$J_S = \frac{V_{max} C}{K_m + C} , \tag{8-6}$$

where V_{max} is a maximum flux per unit membrane area at high substrate concentrations, C, and the K_m is an apparent affinity of substrate for transporter and is the substrate concentration at which the flux is half-maximal. The curve has the shape of a single-site binding relationship or Langmuir adsorption isotherm, an excellent generality. Higher-order relationships in substrate binding to transporter are possible but are uncommon. In the next sections the basis for the expression is explained.

Fig. 8-2 shows the diminution in effective permeability as concentration rises, in accord with Eq. 8-6, with a half-maximal P and flux when the concentration equals the binding site affinity and half the sites are filled. The equation and the graph tell nothing about the influence of the concentration on side 2, so this lack of information suggests that one define the assumptions underlying Eq. 8-6. First, there is accounting for the amount of substrate, so the implicit **Assumption 1** is that the amount of transporter (and therefore the amount of substrate bound to it) is very low compared to the amount of substrate in V_1 or V_2. **Assumption 2** is that the tanks are well stirred, with no depletion layer on side 1 at the membrane and no accumulation layer on the membrane on side 2. Those two assumptions are pretty obvious, but the third one is not: **Assumption 3** is that the rates binding and release of substrate to and from transporter binding site are extremely high so that there is an instantaneous equilibrium at the site, namely:

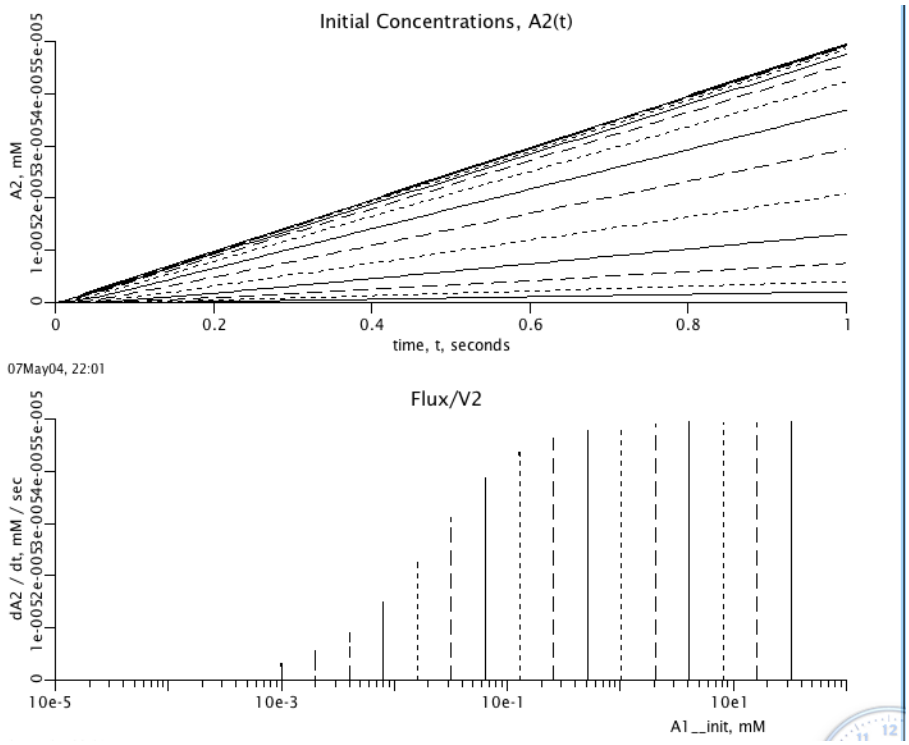

Figure 8-3: Initial transport velocities. A solute with concentration C_1 in volume V_1 permeates the membrane. *Upper panel:* Observations of the time course of concentration C_2 in volume V_2 are made at very early times such that $C_1 \ll C_2$ and C_1 is not measurably depleted by the loss due to the permeation. This is done over a wide range of starting conditions, $C_1(t = 0)$ indicated by the vertical lines in the lower panel. *Lower panel:* The fluxes, $V_2\, dC_2/dt$, are plotted as a function of $C_1(t = 0)$, over a set of initial concentrations from 0.001 mM to over 20 mM. Each starts with a rate near zero since it takes time for substrate to bind to transporter, but at each $C_1(t = 0)$ the rate rises within the first second to the steady-state maximum, the top of each vertical line. At high concentrations the steady-state fluxes (tops of the vertical lines) approach a maximum asymptotically. That the levels of $C_1(t = 0)$ were pushed high enough to reach $V_{\max}$, the maximum velocity of transport, is shown by the fact that at high C_1 the slopes, dC_2/dt in the upper panel, are all the same. REPLACE WITH SIMPLE INIT VELOC

$$K_m = \frac{C \cdot T}{TC} \tag{8-7}$$

Assumption 4 for Eq. 8-6 is that the concentration C_2 is negligible compare to C_1, though of course it must become high enough to be measurable. With these assumptions, one can write the differential equations for the 2-compartment system:

$$\frac{dC_1}{dt} = PS(C_2 - C_1)/V_1 \ , \tag{8-8a}$$

$$\frac{dC_2}{dt} = -PS(C_2 - C_1)/V_2 \quad , \tag{8-8b}$$

$$\text{where } PS = \frac{PS_{max}}{1 + C_1/K_m} \quad . \tag{8-8c}$$

By comparison to Eq. 8-6 we identify $PS_{max} = V_{max}/K_m$. At this point it now becomes evident that there is another assumption, **Assumption 5**: the saturation of the transporter is governed solely by the concentration in compartment 1. And yet this is the commonest version of a transporter equation in general use. Recognizing that the transporter has to be open to both sides of the membrane in order to perform as a transporter, it seems obvious that C_2 should have an equivalent role, so it is natural to account for substrate on both sides of the membrane:

$$PS = \frac{PS_{max}}{1 + C_1/K_m + C_2/K_m} \quad . \tag{8-8d}$$

The consequences of the differing versions of Assumption 5 (Eq. 8-8c versus Eq. 8-8d) are revealed by solving the differential equations.The time course of concentration changes after loading one chamber are shown in Fig. 8-4. Both panels show transients: the concentrations and the fluxes go to zero since there is consumption of substrate in chamber 2. Lines labeled B represent substrate B, with binding to transporter from either side, while substrate A represer case for binding on side on only. In the left panel, the concentration A1diminishes more rap than does B1 whose PS is relatively reduced (Eq. 8-8d instead of Eq. 8-8c). Likewise the unidirectional flux of A1 via the one sided transporter (from V1 to V2) graphed (orange dashe the upper part of the right panel, is much higher than that of B1 (black line), while the net fluxes for A1 and B1 (shown in the bottom section of the right panel in the same colors) are not very different. The code is given in Fig. 8-5; the equations are the standard equation for passive exchange between two compartments but the permeability-surface area product, PS, is calculated at each point in time as the concentrations change.

[Careful examination of the "straight lines" of the upper panel of Fig. 8-3 shows that there is an initial curvature at early times before the line straightens out. Each of the lines can be seen to have a positive intercept on the time axis, e.g. by placing a ruler along any of them between 0.4 and 1.0 seconds; the delay is membrane capacitance due to solute binding to transporter. This is analogous to the delay that was seen in diffusion studies with thick membranes and which produced the intercept L in the Barrer timelag analysis described in Chapter 5 (Barrer, 1953).] The apparent K_m is greater than the actual K_m, a result of a slow binding rate to be elucidated below.

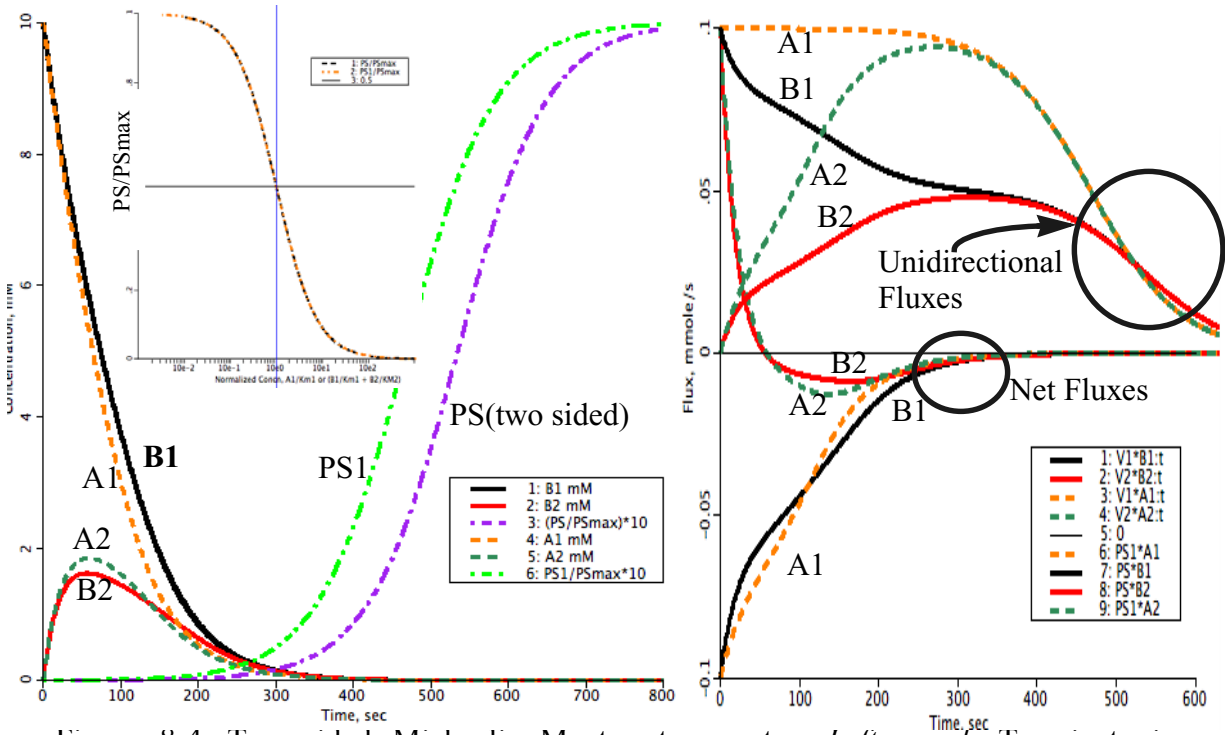

Figure 8-4: Two sided Michaelis Menten transporter: *Left panel*: Transients in concentrations for the one and two-sided transporters. Two sided: with B1(t=0) = 10 mM (black curve) and B2(0) = 0 (red curve) there is a rapid decline in B1(t) while B2(t) rises transiently before the consumption of B2 reduces it gradually to zero. The efflux from V1 is initially nearly maximal (at PSmax*B1) since the transporter is saturated, as indicated by the purple dash-dot curve of PS/PSmax remaining very low for the first 200 seconds. With binding on side 1 only, the concentration on side 1 falls more rapidly (orange dashes, A1) and A2 (dark green dashes) reaches a higher early peak, and the PS1/PSmax (green dash-dot) rises earlier, indicating earlier desaturation of the transporter. Insert panel: The PS/PSmax curves for the two cases are identical for the two cases when plotted against the relevant concentrations, A1/Km1 for the one-sided, and B1/Km1 + B2/Km2 for the 2-sided case. *Right panel*: Net and unidirectional fluxes. Colors and line types as in left panel. The label indicates the nature of the transporter type, B for two sided, and A for 1 sided, the number is the volume source of the flux. The contrast between unidirectional fluxes, A1 compared to B1, and A2 compared to B2 illustrates the magnitudes of the differences, the two-sided, B as substrate) being better. Neither accounts for membrane bound substrate. Parameters set as in Fig. 8-5

8-1.3. Kinetics of facilitated transport with non-instantaneous binding

The process of assisted, or facilitated, permeation of a membrane occurs via binding to special sites on integral proteins (membrane-spanning molecules). The integral protein, the "transporter" has:

— finite abundance, having a total concentration T_T, moles/cm^3 in the membrane;

— variable conformational state allowing the binding site to bind and release substrate at either side of the membrane. Mechanisms vary, but include for example, channel-narrowing behind a transported molecule (Klingenberg, 1981) as in Fig. 8-1.

```
JSim  /* Model TranspMM2:
Short Description: Michaelis-Menten type facilitated transporter
assuming instantaneous solute binding to transporter from either side, case B, or from only side 1, case A.

Description: Transporter-mediated exchange between stirred tanks V1 and V2. The substrate permeates the
membrane via a facilitating saturable Michaelis-Menten type transporter with rapid binding and release at a single
site which is available from either side of the membrane. Two versions are included:
 Substrate A. Cis side driven: Concn A1 determines the fractional saturation, PS/PSmax.
 Substrate B. Cis and trans driven: The governing relative concn is B1/Km1 + B2/Km2.
 Consuming reaction of solute occurs in V2, causing first order disappearance, rate  constant G2.

          _____________________
          |V1    B1(t)        A1 |
          |                      |
          |        ^ PS          |  PS = PSmax/(1 + B1/Km1 + B2/Km2)  ..2 sided
          ---------|------------------|          OR
          |         v            A2  |  PS1 = PSmax/(1 + A1/Km1)   .....................1 sided
          |        B2(t)             |
          |V2          G2            |
          ----------------------------|                                                  */
import nsrunit; unit conversion on;
math TranspMM2 {realDomain t sec; t.min = 0; t.max = 1000; t.delta = 1;

//PARAMETERS
   real  V1  = 1 ml,              // Volume 1
         V2  = 1 ml,              // Volume 2
         PSmax = 20 ml/s,         // PSmax is max
         G2      = 0.035 ml/s,    // Gulosity, first order consumption in V2
         Km1   = 0.005 mM,        // Equilib dissoc const on side 1
         Km2   = 0.005 mM;        // Equilib dissoc const on side 2

// TWO-SIDED BINDING: Substrate B binds Transporter instantly on either side,
// INITIAL CONDITIONS:
  real B1init = 10 mM, B2init = 0 mM, PS(t) ml/s,
       B1(t) mM,      B2(t) mM;       // Solute B concentrations on side 1, side 2;
       when(t = t.min) {B1 = B1init; B2 = B2init;}

// ODEs FOR TWO SIDED BINDING:
      PS  = PSmax / (1+ B1/Km1 + B2/Km2);
      B1:t = - PS * (B1 - B2) / V1;
      B2:t =   PS * (B1 - B2) / V2  - G2*B2 / V2;

// ONE-SIDED BINDING: Substrate A binds Transporter instantly but only on side 1,
  real  A1(t) mM,  A2(t) mM,  PS1(t) ml/s;
  when (t = t.min) {A1 = B1init;  A2 = B2init;}   // Same ICs for A as for B

// ODEs FOR ONE SIDED BINDING MODEL
      PS1  = PSmax / (1 + A1 / Km1);                  // Same PSmax for A as for B
      A1:t = - PS1 * (A1 - A2) / V1;
      A2:t =   PS1 * (A1 - A2) / V2  - G2*A2 / V2;
}
```

Figure 8-5: Michaelis-Menten Transporters: One-sided versus two sided. Code is JSim's MML (mathematical modeling language where A:t represents the derivative dA/dt.

— has highest affinity for substrate molecules of a select type;

The description of the simplest form of transporter begins with a binding reaction following first-order kinetics, solute *S* binding to transporter *T*. This gives a second-order overall reaction when reactions at both surfaces of the membrane and included:

$$S + T \underset{k_{\text{off}}}{\overset{k_{\text{on}}}{\rightleftharpoons}} TS\,.$$

The kinetics for association and dissociation, assuming that subsequent reactions for translocation ar relatively very slow, are written:

$$\frac{dTS}{dt} = k_{\text{on}} \cdot T \cdot S - k_{\text{off}} \cdot TS \tag{8-9a}$$

$$\frac{dS}{dt} = -k_{\text{on}} \cdot T \cdot S + k_{\text{off}} \cdot TS, \tag{8-9b}$$

$$\frac{dT}{dt} = -\frac{dTS}{dt}, \tag{8-9c}$$

where *T*, *TS* and *S* are concentrations of uncomplexed or free transporter, transporter-substrate complex and free substrate, mol cm^3. When the on and off rates are fast compared to the rate of transporter conformational change (flipping), then there is a local equilibrium at each surface:

$$k_{\text{eq}} = \frac{k_{\text{off}}}{k_{\text{on}}} = \frac{T \cdot S}{TS}\,. \tag{8-10}$$

When the equilibrium constant is the same on both sides of the membrane, this simplifies the equations for transport, as in Fig. 8-6. It also introduces a systematic error if it is not exactly true, a point discussed below.

Now consider the two-sided membrane, inside *i* and outside *o,* lying between two stirred media: *six species* (three concentrations on each side of the membrane) and four rate constants (for association and dissociation on each side) are involved. Assuming equilibrium allows TS_{i} to be calculated algebraically from S_{i} and the total concentration of transporter on that side of the membrane, $T_{\text{i}} + TS_{\text{i}}$, such that the ratio in Eq. 8-10 is matched. While $T_{\text{i}} + TS_{\text{i}}$ may change from one moment to the next as S_{i} or S_{o} are changed, the total transporter in the membrane is conserved:

$$\begin{aligned} T_{\text{T}} &= \text{sum of concentration of all transporter forms} \\ T_{\text{T}} &= T_{\text{i}} + TS_{\text{i}} + T_{\text{o}} + TS_{\text{o}}. \end{aligned} \tag{8-11}$$

The unidirectional flux of solute-transporter complex per unit surface area from inside the cell to outside, $J_{\text{TS}_{\text{io}}}$, mol · cm^{-2} s^{-1}, is

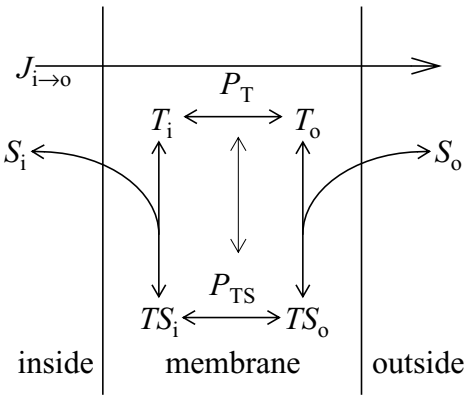

Equilibrium binding:

$$k_d = T_i \cdot S_i / TS_i$$

Carrier concentration in membrane:

$$T_T = T_o + T_i + TS_o + TS_i$$

Solute concentrations: S_i, S_o

Membrane area = A

When $S_o = 0$, for simplicity, then J_{io} the flux per unit membrane area:

$$J_{io} = \frac{P_{TS} T_T / (1 + P_{TS}/P_T)}{2k_d/(1 + P_{TS}/P_T) + S_i} \cdot S_i = \frac{V_{max}}{K_m + S_i} \cdot S_i$$

$\therefore$ Permeability-surface area product, cm^3/s, $PA = \dfrac{V_{max} \cdot A}{K_m + S_i}$;

Rate constant, $sec^{-1} = \dfrac{V_{max} \cdot A}{\text{Volume} \times (K_m + S_i)}$

When $S_o \neq 0$, the transport rate is reduced by the binding of T with S_o:

$$V_{max} = P_{TS} T_T (1 + P' S'_o)/(1 + P' + 2P' S'_o)$$

and

$$K_m = k_d (2 + S'_o + P' S'_o)/(1 + P' + 2P' S'_o)$$

where $P' = P_{TS}/P_T$

and $S'_o = S_o/k_d$

Figure 8-6: Transport via carrier facilitation. Summary of model for single-site binding, with local equilibration between solute, S, and transporter, T at the two surfaces. Two forms are given for J_{io}, one for when the solute concentration, S_o, on the trans (opposite) side of the membrane is zero, and a second, more complex form, when $S_o > 0$.

$$J_{TS_{io}} = P_{TS} \cdot TS_i, \tag{8-12}$$

and the net flux is

$$J_{\text{Net TS}_{io}} = P_{\text{TS}} \cdot (TS_{\text{i}} - TS_{\text{o}}) . \tag{8-13}$$

The flux of total transporter $J_{\text{T}_{io}}$ (in forms T and TS) from inside the cell to outside is the sum for free and complexed transporter:

$$J_{\text{T}_{io}} = P_{\text{T}} T_i + P_{\text{TS}} \cdot TS_i ,$$

and since $TS_i = T_i \cdot S_i / k_{\text{d}}$ from Eq. 8-10, and we define $S'_{\text{i}} = S_{\text{i}} / k_d$ and $S'_{\text{o}} = S_{\text{o}} / k_{\text{d}}$:

$$J_{\text{T}_{io}} = T_{\text{i}} (P_{\text{T}} + P_{\text{TS}} \cdot S'_{\text{i}}) , \tag{8-14}$$

where the concentrations of S are normalized by dividing by the equilibrium dissociation constant k_{eq}, which is assumed here to be the same on both sides.

When the volumes of the solutions on the two sides of the membrane are large enough that transmembrane fluxes change the solution concentrations slowly compared to shifts in the distribution of the transporter with translocation (flips, conformational changes), then, moments after any redistribution a local steady state is reached, and the fluxes of transporter in the two directions must be equal and opposite:

$$J_{\text{T}_{io}} + J_{\text{T}_{oi}} = 0 . \tag{8-15}$$

This is in effect assuming that dS_{i}/dt is much less than either $dT_{\text{T}_{\text{i}}} / dt$ or dTS_{i} / dt occurring with association and dissociation of solute. This simplifications implies that $T_{\text{T}} \ll S$ and that $dS_{\text{i}}/dt \ll dT_{\text{T}}/dt$. This assumption was implicit in the pioneering work of Wilbrandt and Rosenberg, 1961, and Foster and Jacquez, 1975.

Rewriting Eq. 8-15 gives

$$T_{\text{i}} (P_{\text{T}} + P_{\text{TS}} S'_{\text{i}}) - T_{\text{o}} (P_{\text{T}} + P_{\text{TS}} S'_{\text{o}}) = 0 , \tag{8-16}$$

$$T_{\text{i}} = \frac{(P_{\text{T}} + P_{\text{TS}} S'_{\text{o}})}{(P_{\text{T}} + P_{\text{TS}} S'_{\text{i}})} \cdot T_{\text{o}} = \frac{\gamma_{\text{o}}}{\gamma_{\text{i}}} \cdot T_{\text{o}} . \tag{8-17}$$

These γ's have the same units as the P's, i.e., permeability (cm s^{-1}) as defined in Eq. 8-17.

For transporter conservation, from Eq. 8-11,

$$T_{\text{T}} = T_{\text{i}} + TS_{\text{i}} + T_{\text{o}} + TS_{\text{o}} \tag{8-18a}$$

$$= T_{\text{i}} (1 + S'_{\text{i}}) + T_{\text{o}} (1 + S'_{\text{o}}) \tag{8-18b}$$

$$= T_{\text{i}} \delta_{\text{i}} + T_{\text{o}} \delta_{\text{o}} \tag{8-18c}$$

$$\text{and } T_{\text{i}} = \frac{T_{\text{T}}}{\delta_{\text{i}}} - T_{\text{o}} \frac{\delta_{\text{o}}}{\delta_{\text{i}}} . \tag{8-18d}$$

The δ's defined in Eqs. 8-18a to 8-18d are scalars (dimensionless) that are governed by the solute concentrations and the equilibrium dissociation constants. Combining Eqs. 8-17 and 8-18a to 8-18d:

$$\frac{\gamma_o \cdot T_o}{\gamma_i} = T_i = \frac{T_T}{\delta_i} - T_o \cdot \frac{\delta_o}{\delta_i}, \tag{8-19a}$$

$$T_o = T_T \cdot \frac{\gamma_i}{\gamma_o \delta_i + \gamma_i \delta_o}, \tag{8-19b}$$

$$T_i = T_T \cdot \frac{\gamma_o}{\gamma_o \delta_i + \gamma_i \delta_o}, \tag{8-19c}$$

from which one calculates the unidirectional fluxes for the solute-transporter complex, which is the same as that for the solute (and assuming Eq. 8-10, $TS_i = T_i \cdot S_i/k_{eq} = T_i S'_i$):

$$J_{io} = P_{TS} \cdot TS_i = T_T \cdot \frac{\gamma_o}{\gamma_o \delta_i + \gamma_i \delta_o} \cdot (P_{TS} \cdot S'_i), \tag{8-20a}$$

$$J_{oi} = P_{TS} \cdot TS_o = T_T \cdot \frac{\gamma_i}{\gamma_o \delta_i + \gamma_i \delta_o} \cdot (P_{TS} \cdot S'_o) \quad . \tag{8-20b}$$

From Eq. 8-20a, the effective conductance P_{eff} for the unidirectional efflux, J_{io}, of solute is

$$P_{eff}(J_{io}) = \frac{T_T P_{TS} \cdot \gamma_o}{\gamma_o \delta_i + \gamma_i \delta_o}. \tag{8-21}$$

The net efflux per unit surface area is

$$J_{Netio} = J_{io} - J_{oi}. \tag{8-22}$$

8-1.4. Unidirectional flux with zero transconcentration

With $S_o = 0$ the expression for efflux simplifies since $\gamma_o \to P_T$ and $\delta_o \to 1$. Regrouping terms in Eq. 8-20a and using P' for P_{TS}/P_T:

$$J_{io} = \frac{T_T P_{TS} S'_i}{2 + S'_i(1 + P')} \tag{8-23a}$$

$$= \frac{T_T \cdot \dfrac{P_{TS}}{1 + P'} \cdot S_i}{2k_{eq}/(1 + P') + S_i}. \tag{8-23b}$$

When $P_{TS} = P_T$, both forms of the carrier having equal likelihood to flip to the opposite side, then

$$J_{io} = \frac{\frac{1}{2}T_T \cdot P_{TS} \cdot S_i}{k_d + S_i}. \tag{8-24}$$

This is the standard "Michaelis-Menten"-like first-order expression for an enzymatic reaction, now applied to carrier transport, using V_{max} as the maximum transport rate and K_m as the "apparent Michaelis constant", and where $K_m = K_d$ when the binding-unbinding is infinitely fast:

$$J_{io} = \frac{V_{max} S_i}{K_m + S_i}. \tag{8-25}$$

Thus for Eqs. 8-23a and 8-23b, we see that

$$V_{max} = T_T \cdot P_{TS} / (1 + P'), \tag{8-26a}$$

$$K_m = 2k_d / (1 + P') . \tag{8-26b}$$

Figure 8-7 provides some useful clues as to overall behavior.

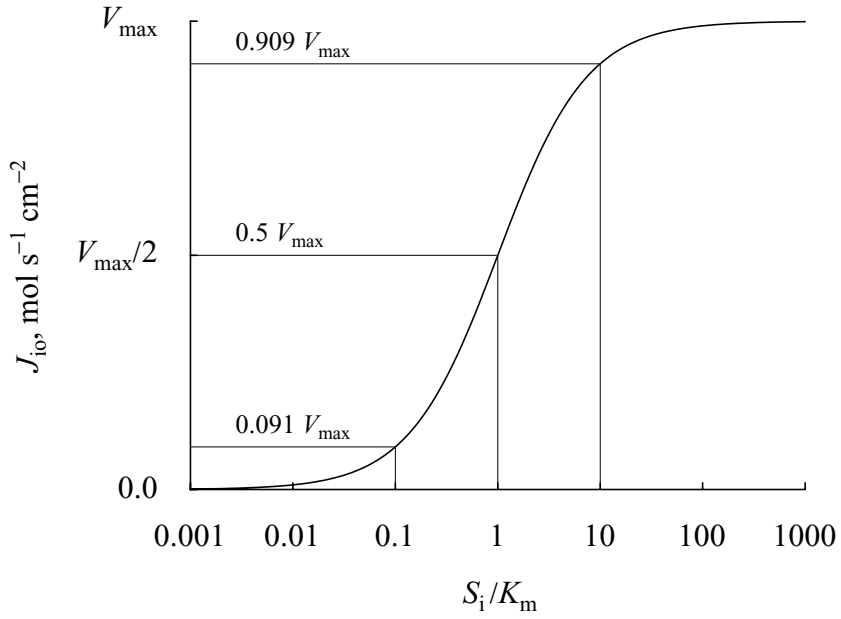

Figure 8-7: Saturation kinetics with a facilitating transporter.

1. When $S_i = K_m$, the flux is half-maximal: $J_{io} = V_{max}/2$.
2. When $S_i = 10K_m$ and $100K_m$, then $J_{io} \approx$ 90.9% and 99% of V_{max}.
3. When $S_i = 0.1K_m$ and $0.01K_m$, then $J_{io} \approx$ 9.1% and 1% of V_{max}.
4. The slope $dJ_{io}/d(S_i/K_m)$ is $V_{max}/(1 + S')^2$. It is steepest at the inflection point $S_i = K_m$, where it is $V_{max}/4$.
5. At low substrate concentrations, $S_i \ll K_m$, the process is first order, $J_{io} = V_{max}/K_m$.

6. There are four unknown parameters in Eq. 8-26a and 8-26b. It is clear that the combination $T_T P_{TS}$ always appears as a product and these are therefore inseparable kinetically. Likewise $(1 + P')$ is always combined with another term.

Thus, raising the concentration S_i fills the binding sites and the transport efflux rises to a maximum when all the sites on the inside, side i, are occupied all the time.

The effective permeability for the solute is therefore a concentration-dependent value, as is shown in Fig. 8-8, and is

$$P_{eff} = \frac{T_T \cdot P_{TS}/(1 + P')}{2k_d/(1 + P') + S_i}. \tag{8-27}$$

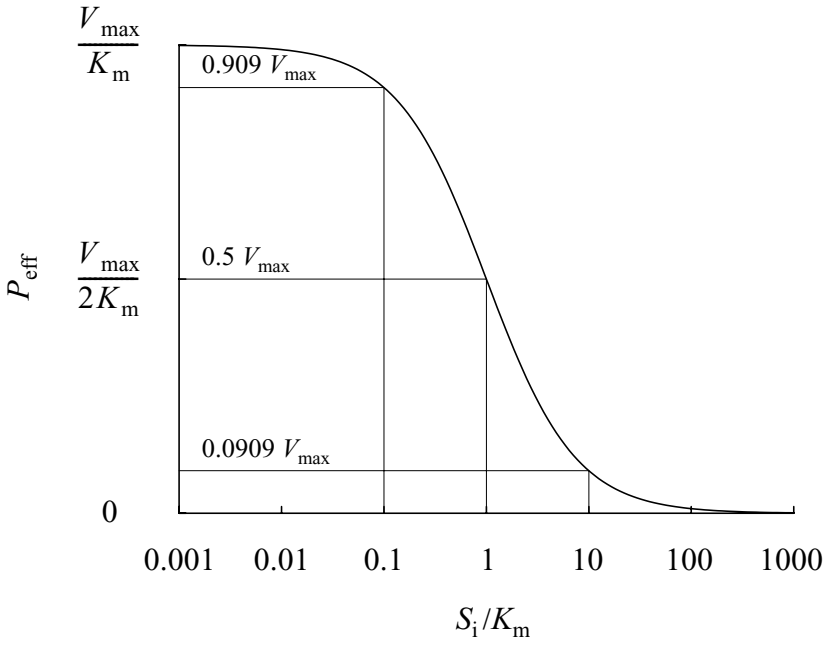

Figure 8-8: Effective permeability for unidirectional flux for a saturable transporter.

The case where $P_{TS} = P_T$, or $P' = 1$, is a common case since the solute molecule does not often influence the rate of conformational change.

$$J_{io} = \frac{T_T \frac{P_{TS}}{2} \cdot S_i}{k_d + S_i}, \tag{8-28a}$$

$$\text{where } V_{max} = \frac{1}{2} T_T P_{TS} \tag{8-28b}$$

$$\text{and } K_m = k_d . \tag{8-28c}$$

This is now the standard Michaelis-Menten transporter expression; it explicitly identifies V_{max} as the product of $T_T/2$ (since half of the transporter faces each side of the membrane) times the rate of conformational change, P_{TS}. The trans-concentration has no influence on J_{io} when $P_{TS} = P_T$ and affinity is the same on both sides, $k_{d_i} = k_{d_o}$. The effective P_{eff}, for the case when $P' = 1$, diminishes as S_i is increased (and is also diminished by increasing S_o):

$$P_{eff}(P' = 1) = \frac{V_{max}}{K_m + S_i} = \frac{\frac{1}{2}T_T P_{TS}}{k_d + S_i}. \tag{8-29}$$

Note the similarity in the shape of PS in Fig. 8-8 to that of the volume of distribution for a solute-specific binding site as shown in Chapter 10, Fig. 10.5. The effective volume of distribution and the effective transporter PS diminish at higher substrate concentrations for the same reason—at higher S_i fewer binding sites are available.

At very low S_i where $S_i'(1 + P_{TS}) \ll 2$, the S_i in the denominator becomes negligible and Eqs. 8-23a and 8-23b reduce to

$$J_{io} = \frac{T_T \cdot P_{TS}}{2k_d} \cdot S_i. \tag{8-30}$$

This is now a *linear equation* with an apparent or effective permeability $P_{eff} = T_T \cdot P_{TS}/2k_d$ and is independent of S_i, so long as $S_i < 0.01\ k_d$.

8-1.5. Transporter equations allowing for slow binding and release:

In the preceding section the reduction to the algebraic equations was based on the assumptions that: (1) the solute binding and unbinding reactions were fast compared with the translocation of the substrate-transporter complex, and (2) the transporter concentration is small compared with that of the substrate. When that is not the case there are then six molecular species to consider, namely the solute concentrations on the two sides of the membrane, and the two forms of the transporter, free and complexed with solute, on each side, as follows in Eqs. 8-31a to Eqs. 8-31g:

$$\frac{dS_1}{dt} = -k_{on1} \cdot T_1 \cdot S_1 + k_{off1} \cdot TS_1 , \tag{8-31a}$$

$$\frac{dT_1}{dt} = -k_{on1} \cdot T_1 \cdot S_1 + k_{off1} \cdot TS_1 - k_{T12} \cdot T_1 + k_{T21} \cdot T_2 \tag{8-31b}$$

$$\frac{dTS_1}{dt} = k_{on1} \cdot T_1 \cdot S_1 - k_{off1} \cdot TS_1 - k_{TS12} \cdot TS_1 + k_{TS21} \cdot TS_2 , \tag{8-31c}$$

$$\frac{dTS_2}{dt} = k_{on2} \cdot T_2 \cdot S_2 - k_{off2} \cdot TS_2 + k_{TS12} \cdot TS_1 - k_{TS21} \cdot TS_2 , \tag{8-31d}$$

$$\frac{dT_2}{dt} = -k_{on2} \cdot T_2 \cdot S_2 + k_{off2} \cdot TS_2 + k_{T12} \cdot T_1 - k_{T21} \cdot T_2 \quad , \tag{8-31e}$$

$$\frac{dS_2}{dt} = -k_{on2} \cdot T_2 \cdot S_2 + k_{off2} \cdot TS_2 \quad . \tag{8-31f}$$

with the constraint that

$$T_{tot} = T_1 + T_2 + TS_1 + TS_2 = \text{a constant} \quad , \tag{8-31g}$$

so that the equation for T_2 can be replaced by $T_2 = T_{tot} - TS_1 - T_1 - TS_2$.

From the thermodynamic point of view there is another constraint that applies when the system is not coupled to an energy source, namely the Haldane constraints that apply to any reversible chemical reaction. For a passive transporter, the transport rate constants should satisfy the following:

$$\frac{k_{TS12} \cdot k_{T21} \cdot k_{on1} \cdot k_{off2}}{k_{TS21} \cdot k_{T12} \cdot k_{off1} \cdot k_{on2}} = 1 \tag{8-32}$$

These constraints ensure that the model runs to equilibrium at steady-state. If the ratio deviates from 1, the model will run to a steady-state net concentration gradient. This could be the case if the transporter is coupled to an energy source, which is not explicitly modeled here. A solution is provided in Fig. 8-9 for the system with the only substrate initially being A1.

Model Inputs		
V1	1	ml
V2	1	ml
Surf	1	cm^2
Ttot	1E-5	umol/cm^2
KdA1	0.1	uM
KdA2	0.1	uM
konA1	1000	uM^-1*s^-1
konA2	1000	uM^-1*s^-1
kT12	1	s^-1
kTA12	1	s^-1
kT21	kT12	s^-1
kTA21	kTA12	s^-1
A1__init	0.001	mM
A2__init	0	mM
TA1__init	0	umol/cm^2
TA2__init	0	umol/cm^2

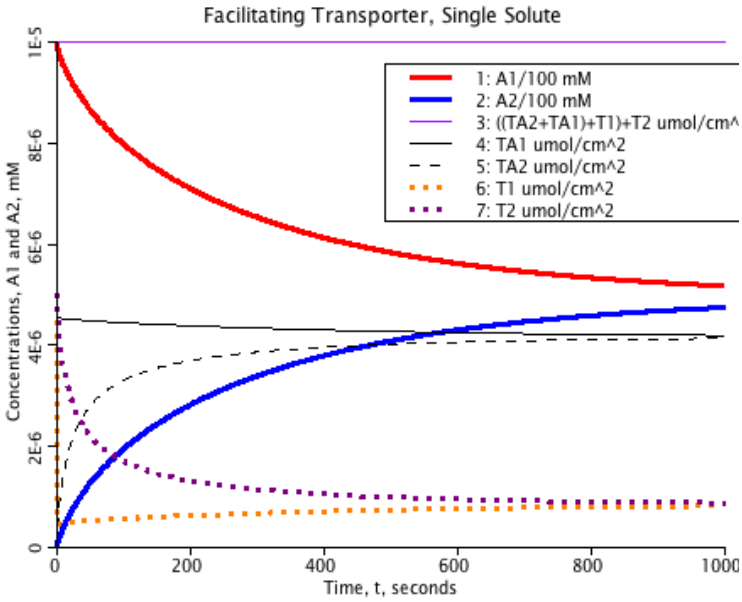

Figure 8-9: Transporter kinetics with finite rate of binding. Note that $A_1(t=0)$ = 1 µM, only 10 times the k_{dA1}. A_1 equilibrates with A_2 at over 3000 seconds, but at a value less than 0.5 $A_1(t=0)$, namely 0.496 $A_1(t=0)$, because some A is attached to the transporter sites, 80% of which are occupied, as TA_1 and TA_2. The sum of the 4 transporter forms is constant.

The code for a transporter (Figure 8-10) that may bind with either one of two competing

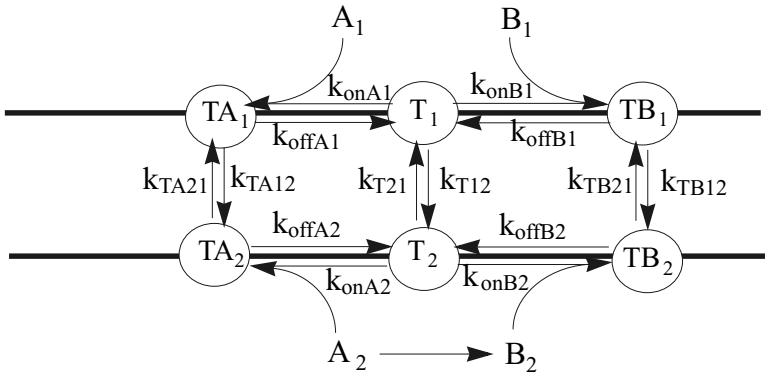

Figure 8-10: Diagram of a transporter carrying either of two solutes. Solute A reacts to form B only on side 2. Equations in MML code are in Table 8-1.With solutes A and B in competition for the binding site on the same side of the membrane, the presence of one inhibits the transport of the other. When the probabilty of flipping the active site from one side to the other is less for unbound transporter than for bound transporter (the k_Ts < the k_{TA}s or k_{TB}s), then when $A_1 > A_2$ there is facilitation of transport of B_2 to B_1. With $K_{T12} = K_{T21} = 0$, there is obligatory countertransport..

substrates, A and B, is shown, with units, in Table 8-1. The results in Fig. 8-9 for the single solute

Table 8-1: facT2, two solutes competing for the transport site (JSim MML code)

```
JSim v1.1   // Facilitating transporter: 2 competing solutes with binding steps, converts A2 to B2
            // Demonstrates countertransport facilitation or inhibition
import nsrunit; unit uM = 1e-6 M; unit conversion on;
math facT2 {realDomain t sec; t.min = 0; t.max = 30; t.delta = 0.1;
//PARAMETERS:
real V1  = 1 ml,                    //Volume 1
     V2  = 1 ml,                    //Volume 2
     Surf= 1 cm^2,                  //Surface area for exchange
     Ttot= 1 umol/cm^2;             //Transporter conc per unit surf area
real KdA1  = 10 uM,                 KdA2 = 10 uM,            //Equilib dissoc const on each side, solute A
     KdB1  = 10 uM,                 KdB2 = 10 uM,            //Equilib dissoc const on each side, solute B
     konA1 = 1 uM^(-1)*s^(-1),  konA2 = 1 uM^(-1)*s^(-1),    // on rates, solute A
     konB1 = 1 uM^(-1)*s^(-1),  konB2 = 1 uM^(-1)*s^(-1),    // on rates, solute B
     koffA1 = KdA1*konA1,       koffA2 = KdA2*konA2,         // off rates s^(-1) solute A
     koffB1 = KdB1*konB1,       koffB2 = KdB2*konB2,         // off rates s^(-1) solute B
     kT12  = 100 s^(-1),        kT21  = 100 s^(-1),          // free transporter flip rate 1->2 & 2->1
     kTA12 = 100 s^(-1),        kTA21  = 100 s^(-1),         // TA flip rates
     kTB12 = 100 s^(-1),        kTB21  = 100 s^(-1),         // TB flip rates
     KmA2  = 0.4 mM,                                         // Km for consump of A in V2
     GmaxA2= 0.1 umol/min,                                   // consump A, Vmax for A to B reaction
     ConsumpA2(t) umol*min^(-1);                             // Consumption rate

// STATE VARIABLES:
real A1(t) mM, A2(t) mM,        B1(t) mM, B2(t) mM,   // Solute concns
     TA1(t) umol/cm^2,          TA2(t) umol/cm^2,     // TA concns
     TB1(t) umol/cm^2,          TB2(t) umol/cm^2,     // TB concns
     T1(t)  umol/cm^2,          T2(t)  umol/cm^2;     // Free transporter concns
// INITIAL CONDITIONS:
when(t=t.min) {A1 = 10; A2 = 0; B1 = 0; B2 = 0;TA1= 0; TA2 = 0; TB1 = 0;TB2 = 0;T1 = 0.5*Ttot; }
// ODEs
A1:t    = Surf*(- konA1*A1*T1/V1 + koffA1*TA1/V1 );   // A1 binds free T1 and TA1 dissociates
ConsumpA2 = GmaxA2 * A2 /(KmA2 + A2);                 // enz.facilitated reaction A 2-> B2
A2:t    = Surf*(- konA2*A2*T2/V2 + koffA2*TA2/V2 )  - ConsumpA2 / V2;  // last term is loss of A -> B
B1:t    = Surf*(- konB1*B1*T1/V1 + koffB1*TB1/V1 );     // B1 binds free T1 and TB1 dissociates
B2:t    = Surf*(- konB2*B2*T2/V2 + koffB2*TB2/V2)  + ConsumpA2 / V2; // last term is formation of B
T1:t    = - (konA1*A1 + konB1*B1)*T1 + koffA1*TA1 + koffB1*TB1 - kT12*T1 + kT21*T2;
TA1:t =  konA1*A1*T1 - koffA1*TA1    - kTA12*TA1  + kTA21*TA2;  // first term is association
TA2:t =  konA2*A2*T2 - koffA2*TA2    + kTA12*TA1  - kTA21*TA2;  // 2nd term is dissociation
TB1:t =  konB1*B1*T1 - koffB1*TB1    - kTB12*TB1  + kTB21*TB2;  // 3rd term is transport 1 -> 2
TB2:t =  konB2*B2*T2 - koffB2*TB2    + kTB12*TB1  - kTB21*TB2;  // 4th term is transport 2 -> 1
T2      = Ttot - TA1 - TA2 - TB1 - TB2 - T1;                    //  Conservation of transporter.
 }
```

may be reproduced by using this code and setting the concentrations of B to zero and the other parameters as in Fig. 8-9. (This code will be used in the next section too.)

8-2. Countertransport facilitation

When two solutes are transported by the same transporter (Figure 8-10), they compete for the bindiing site, thus inhibitng one another. An interesting practical example, here presented as an analog to the experiments of Wilbrandt and Rosenberg (1954??) or those of (??? on glucose) is shown in Figure 8-11 . It shows the coupling of transport for the two solutes, the phenomenom of countertransport, which is defined as the facilitation of transport of solute B from side 2 to side 1 by the transport of solute A from side 1 to side 2, and vice versa. When $A_1 > A_2$ there is a driving force (the concentration gradient for solute A), even when k_{TA12} and k_{TA21} are equal, for the delivery of unbound transporter, T_2, to side 2, making it available for binding to B_2 and carrying back to side 1. In the situation in Figure 8-11 , solute B is formed only from A on side 2, but the

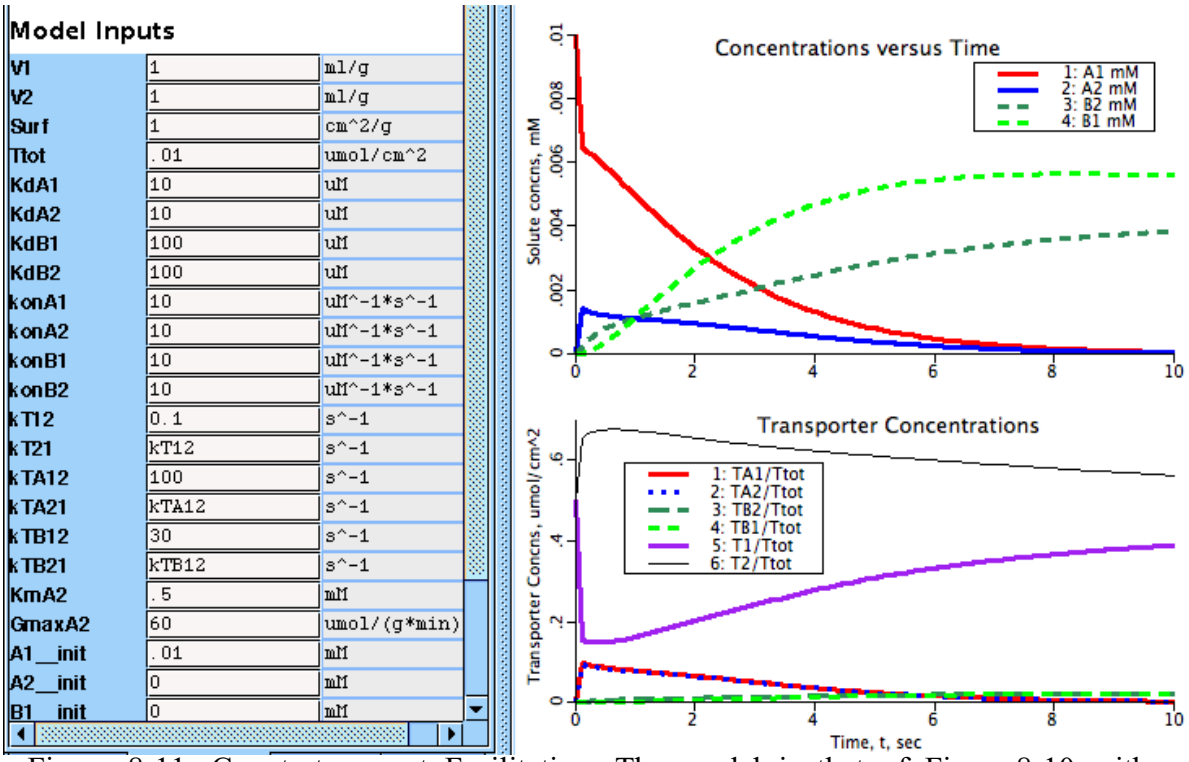

Figure 8-11: Countertransport Facilitation. The model is that of Figure 8-10 with parameter values shown on the left column. B is fromed from A on side 2. The sharp drop in A1 is due to the binding of A to transporter, raising the concentration of TA_1 rapidly; that of TA_2 follows quickly, depending on the value for k_{TA12}. The transport of A in the form of TA from side 1 to side 2 delivers, after dissociation TA_2 , unbound T to side 2 and drives B from side 2 to side 1, raising the concentration B_1.

countertransport facilitation is so strong that B_1 is raised higher than B_2.contrary to expectations from the energy gradient or chemical potential difference for B. So long as the flux of unbound transporter is not zero, with both k_{T12} and k_{T21} non-zero, *and* there is a driving force for A1 to A2, then B1 remains higher than B2. However when A is fully consumed, then B1 and B2 will equilibrate. Note that the binding affinities in this example are the same on the two sides of the membrane. The facilitation occurs even though the affinities for B might be higher or lower than

for A, but depends most on the condition that the fluxes of unbound T are at lower rates than for TA of TB. If $k_{T12} = k_{T21} = 0$, then this is an obligatory transporter, similar functionally to the NaH exchanger and the NaCa exchanger, neither of which are dependent upon ATP.

The effect of slow binding on the apparent K_d: When the rate of binding of free solute A1 to the tranpsorter is slow, the curvature and delay of the intercept for the curves in Fig. 8-3 is greater for small initial concentrations, $A_1(t = 0)$, than for large concentrations because the relative amount held on the binding sites is less at high concentrations. There is an additional effect of slow binding, the rightward (upward) shift in the apparent K_d. Furthermore there is a increase in the steepness of the slope of the relationship between flux and concentration, mimicking an increased (but false) degree of cooperativity. In Fig. 8-12 are plotted the fluxes in Fig. 8-3 versus the initial concentrations. The fluxes are proportional to the slopes after a pseudo-steady state has been reached. This has to be termed "pseudo" since at substantially later times the slope diminishes because when A_2 becomes non-negligible and there is backflux into A_1. The curves of $A_2(t)$ are, since the flux is into a fixed volume, the first part of a nearly exponential curve. The steady state fluxes are close to the expected sigmoidal relationship typical of Michaelis -Menten transporters with a half-maximal rate at the K_d and a logarithmic slope of 1.0.

8-3. Application to tracer experiments on capillary permeability

To determine the K_m and V_{max} for a transporter on the luminal surface of the endothelial cell, a series of multiple tracer indicator dilution experiments to estimate the fractional extraction of tracer at each of several background levels of non-tracer S_i. Then the permeability surface area product $P_{eff}A$, and V_{max} and K_m are estimated by optimizing the fit of Eq. 8-25 to the data. An example is shown in Fig. 8-13.

This process provides estimates of K_m and V_{max} (Eqs. 8-26a and 8-26b) but these cannot be parsed to provide P', nor can one separate the components of $T_T P_{TS}$. Another set of experiments, with $S_o > 0$ is required to estimate P'. No transient tracer experiment will separate T_T from P_{TS}—an increase in the number of transporters is as effective in increasing P_{eff} as is an increase in P_{TS}. Measurement of the concentration of the specific transporter protein by antibody labeling is one way to estimate T_T. The growing efforts to characterize the "proteome", the nature and quantity of all cellular proteins, are beginning to provide data on intracellular enzyme concentrations; changing concentrations are taken to be evidence of genetic regulation or changing rates of proteolysis. These are a part of what Kuile and Westerhoff (2002) entitle "hierarchical regulation" of metabolic flux, to contrast it with substrate-supply-driven "metabolic regulation".

There are potential sources of error in such experiments. The likeliest problem is that perfusing the heart with a solution of adenosine is likely to change the physiological state, reducing the vascular resistance and possibly reducing the strength of contraction. The biggest worry, however, is that having a high capillary concentration will cause a raised intracellular concentration and then influence the apparent P_{eff} by inducing countertransport facilitation or inhibition, if the relevant parameters of the system P_{TS} and P_T differ. The results in Fig. 8-13 show no evidence of a systematic deviation from Eq. 8-25: if there were facilitating countertransport then the data would lie above the theoretical curve at high concentrations and would fall below it if there were inhibitory countertransport. A reasonable conclusion is that $P' = 1$ for the purine

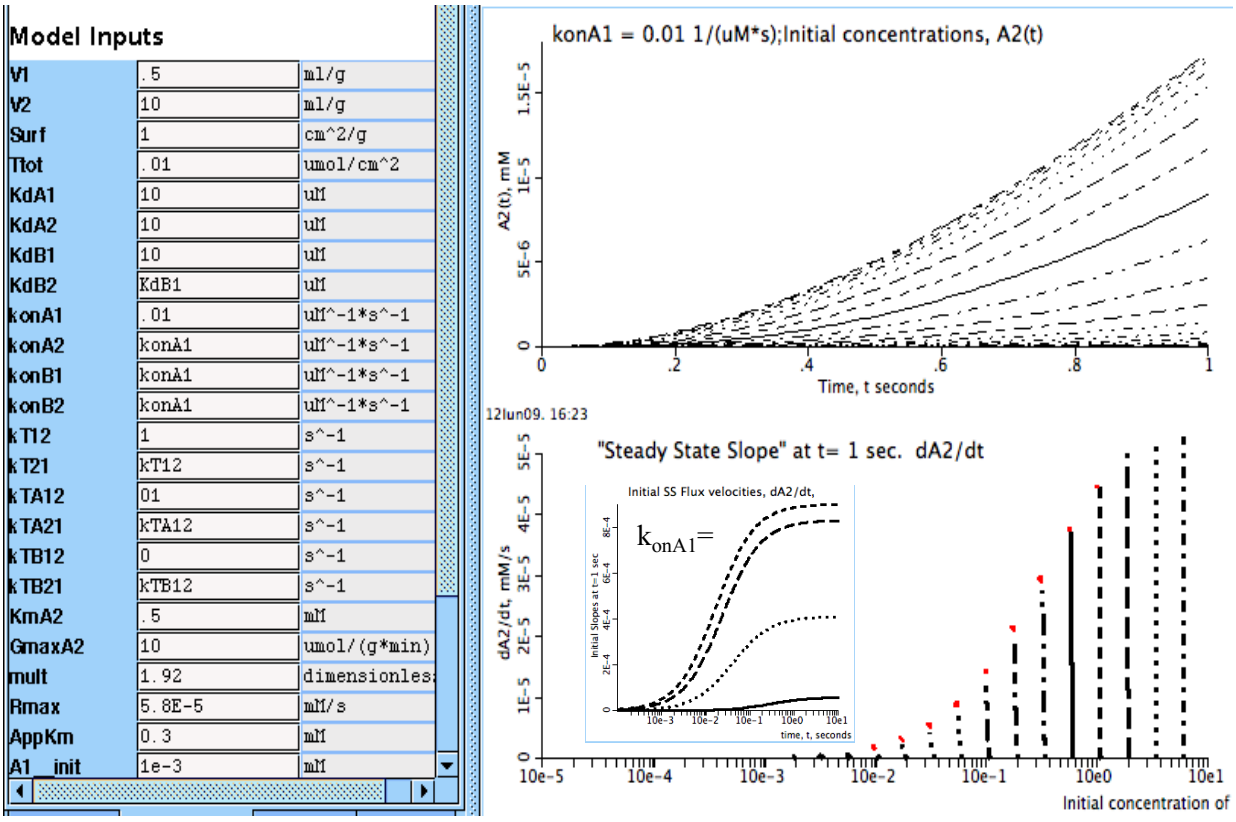

Figure 8-12: The effect of slow binding rate on the k_{onA1}= 100 $(mM*s)^{-1}$ R_{max} = 9.0e-4, and AppKm = 0.017 mM "pseudo-steady state" fluxes as a function of initial concentrations in the initial velocity experiments portrayed in Fig. 8-3. *Upper Panel:* Initial concentrations $A_2(t)$, showing initally depressed rates of transfer across the membrane due to the slow binding of A_1 to the transporter. *Lower Panel:* At a fast rate of binding, 10 $mM^{-1}s^{-1}$ the theoretical Michaelis-Menton relationship betgween flux and concentration is almost obeyed. However at the slower rates the fluxes are reduced in magnitude and the concentration achieved by the end of the 1 second of the upper panel are less than the expected curve. In the lower panel these are represented by the tops of the lines of the sequence of values of dA_2/dt plotted for each initial concnetration, $A_1(t=0)$. The apparent half-maximal rate is shifted to the right, to higher concentrations (mimicking a lower affinity), but the slope of change of flux per scalar increase in concentration is unchanged. The flux curves in the insert panel (lower) shift rightward and have lower maxima when k_{onA1}, the rate constant for binding, is lowered. The red dotted curve in *lower panel* and the 4 curves in the *Insert Panel* are the maximum fluxes at high concentrations at the end of 1 s, R_{max}, and are fitted by Flux = $R_{max}\ A_1/\ (AppK_m + A_1)$:

k_{onA1}= 100 $(mM*s)^{-1}$ R_{max} = 9.0e-4, and AppKm = 0.017 mM
k_{onA1}= 1 $(mM*s)^{-1}$ R_{max} = 8.3e-4, and AppKm = 0.024 mM
k_{onA1}= 0.1 $(mM*s)^{-1}$ R_{max} = 4.1e-4, and AppKm = 0.04 mM
k_{onA1}= 0.01 $(mM*s)^{-1}$ R_{max} = 5.8e-5, and AppKm = 0.3 mM

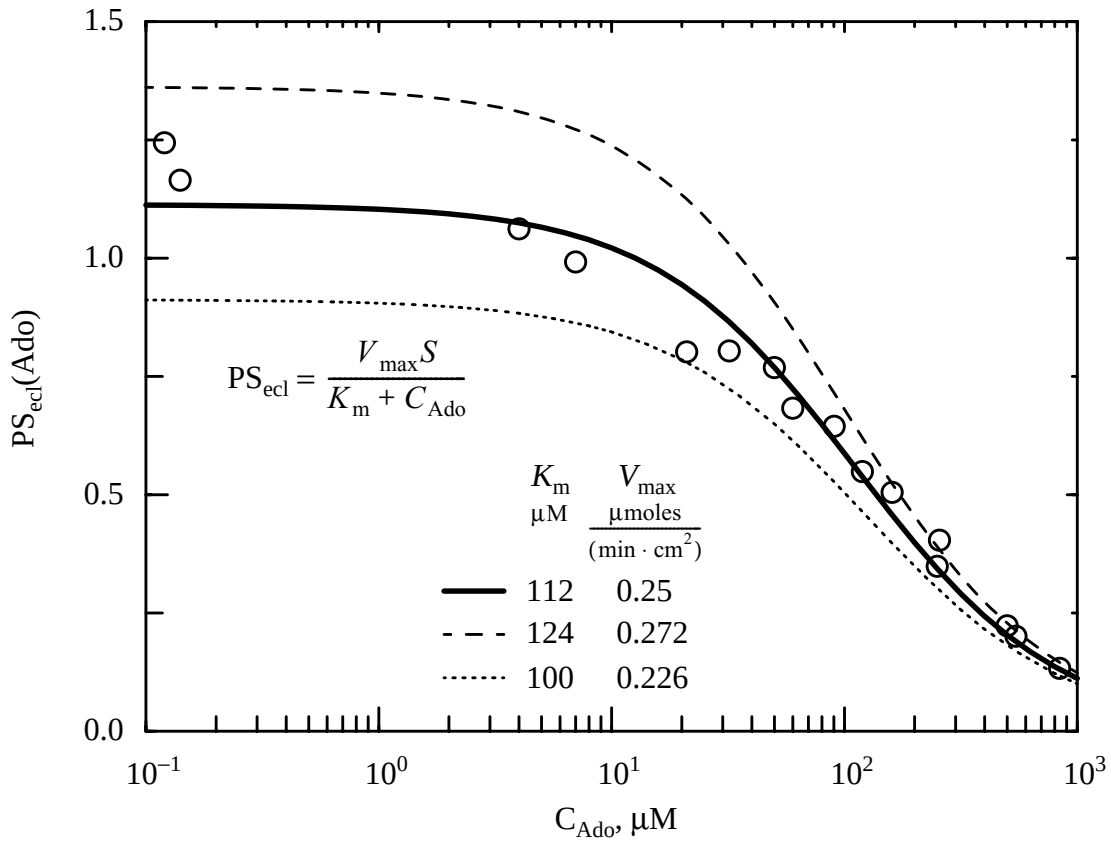

Figure 8-13: Estimated PS_{ecl} (open circles) versus venous effluent adenosine concentrations, C_{Ado}. From this, the parameters for the nucleoside transporter on the luminal surface of coronary capillary endothelial cells were estimated using nonlinear least squares optimization assuming Michaelis-Menten kinetics. This gave $K_m = 112 \pm 12$ μM and $V_{max} = 0.25 \pm 0.023$ μmoles min^{-1} cm^{-2} and $PS_{eclMax} = 1.12$ ml g^{-1} min^{-1} for the adenosine transport, where the ± values represent the 95% confidence limits. (Data from Krebs-Henseleit perfused guinea pig hearts. From Schwartz et al., 2000, with permission from the American Physiological Society.)

nucleoside transporter in cardiac endothelial cells, as has been thought to be the case for erythrocytes (Plagemann and Wohlhueter, 1980). Cases for $P' \neq 1$ are considered next.

8-3.1. Unidirectional flux with finite trans concentration (facilitation and Inhibition)

Adding substrate to the trans side so that $S_o > 0$ changes the cis-to-trans flux, J_{io}. When $P_{TS} > P_T$, this gives *facilitating countertransport,* cis-to-trans flux is raised. (*Cis* is this side, *trans* is the other side; thus we are considering *cis* as *inside*.) The reason is that by raising S_o, converting more T_o to TS_o, more carrier is returned from trans to cis, making more transporters available on the cis side for cis-to-trans flux. This is summarized by saying that raising S_o raises γ_o in Eq. 8-20a. *Inhibitory countertransport* occurs when $P_{TS} > P_T$ so that raising S_o decreases J_{io}.

Figure 8-14 illustrates the effect of S_o on J_{io}: the effective membrane P_{eff} for cis to trans flux, J_{io}, as is given by Eq. 8-21, for any S_o. From this, simplified cases are derived from Eq. 8-20a:

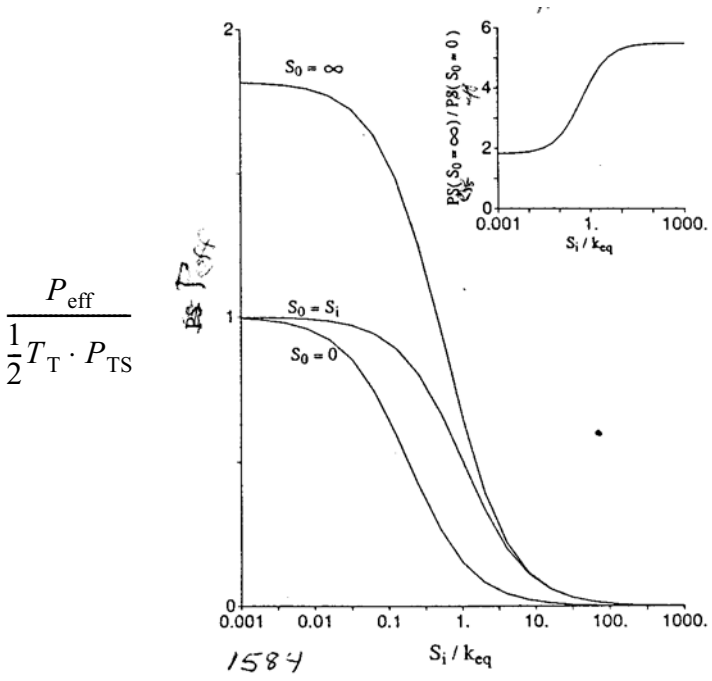

[The inset is Eq. 13.26]

[Redraw using 13.22, .23, .24]

Figure 8-14: Facilitating Countertransport. With $P_{TS}/P_T = P' = 10$, the effect of raising the outside concentration S_o is to increase the P_{eff} and the unidirectional flux from inside to outside. In general $P' > 1$ gives countertransport facilitation because the transporter returns more quickly to the cis side when it is occupied by substrate from the trans side.

$$\text{when } S_o = 0\text{: } P_{eff} = \frac{(1/2)T_T \cdot P_{TS}}{k_{eq} + S_i(1 + P_{TS}/P_T)/2}, \tag{8-33}$$

$$\text{when } S_o = S_i\text{: } P_{eff} = \frac{(1/2)T_T \cdot P_{TS}}{k_{eq} + S_i}, \tag{8-34}$$

$$\text{when } S_o = \infty\text{: } P_{eff} = \frac{(1/2)T_T P_{TS}}{(k_{eq}/2)(1 + 1/P') + S_i}. \tag{8-35}$$

When $P' = 1$, these all reduce to the same form:

$$P_{eff}(S_o = 0) = P_{eff}(S_o = S_i) = P_{eff}(S_o = \infty) = \frac{(1/2)T_T \cdot P_{TS}}{k_{eq} + S_i}, \tag{8-36}$$

which is the same as Eq. 8-24. In Fig. 8-14 one can see the effects of P_{TS} being greater than P_T: the apparent K_m is shifted to the left for both extreme cases, $S_o = 0$ and $S_o = \infty$. However, the relative effects of $S_o = \infty$ versus $S_o = 0$ depend on S_i:

$$\frac{P_{\text{eff}}(S_{\text{o}} = \infty)}{P_{\text{eff}}(S_{\text{o}} = 0)} = \frac{2/(1 + P') + S'_{\text{i}}}{\frac{2}{1 + P'} \cdot \left[\frac{1}{2} \cdot (1 + 1/P') + S'_{\text{i}}\right]} . \tag{8-37}$$

This is plotted in the insert in Fig. 8-14. For example, at $S'_{\text{i}} = 1$ and $P' = 10$ as in Fig. 8-14 (insert),

$$P_{\text{eff}}(S_{\text{o}} = \infty)/P_{\text{eff}}(S_{\text{o}} = 0) = \frac{3 + P'}{3 + 1/P'} = \frac{13}{3.1} = 4.19 . \tag{8-38}$$

Note that the ratio at $S'_{\text{i}} = 1$ is not at the mid level between the plateaus at low S'_{i} and high S'_{i} but is a little higher; this is because the apparent K_{m}'s are different in the two cases:

$$K_{\text{m}}(S_{\text{o}} = 0) = 2k_{\text{eq}}/(1 + P') = 0.18\ k_{\text{eq}} ,$$

$$K_{\text{m}}(S_{\text{o}} = \infty) = \frac{k_{\text{eq}}}{2}(1 + 1/P') = 0.55\ k_{\text{eq}} .$$

8-4. Tracer transients with saturable transport

8-5.1. Tracer Unidirectional fluxes during Steady State of partial saturation

8-5.2. Tracer fluxes during transients in mother solute fluxes (bolus sweep)

Crone (1965) showed that the effective P for tracer-labelled D-glucose in the brain was reduced by raising the blood glucose level, thereby providing direct evidence for flux mediation by a saturable transporter. The experiment was based on the principle that the injection of a bolus of tracer glucose had no effect on the apparent P_{eff}, but that the non-tracer glucose level controlled P_{eff} in accord with Eqs. 8-23a and 8-23b. (Experimentally, it is therefore important that the tracer be of high specific activity so that additional non-tracer content in the injectate is negligible.)

Linehan et al. (1987) introduced the "bolus sweep" technique, an experimental approach in which non-tracer is injected simultaneously with non-tracer mother solute in order to create a transient during which there is a changing degree of competition between non-tracer and tracer. Mother solute, the same species as the tracer but with no tracer label, competes with tracer for the transporter binding site. The P_{eff} therefore changes as a function of time as shown in Fig. 8-15, where P_{eff} diminishes as the plasma concentration of non-tracer rises to the peak within the capillary, and then P_{eff} rises again as the bolus washes out of the capillary. The effects on the tracer extraction are shown in Fig. 8-16. In this case the non-tracer concentration was nearly zero at the earliest part of the bolus, so there was no competition from non-tracer to inhibit binding of tracer to the transporter initially. When the peak bolus concentration was inside the capillary the tracer transport was about three-quarters inhibited, as shown by the reduction in the instantaneous extraction, $E(t) = 1 - h_{\text{D}}(t)/h_{\text{R}}(t)$, as the bolus sweeps past the transporter sites on the capillary endothelium.

An experiment done by Dawson et al. (1984) on the endothelial uptake of PGE_1 (prostaglandin E_1) is shown in Fig. 8-17. PGE_1 is taken up but almost none is released to return to the capillary blood, so the values of $E(t)$ again approach the maximum during the tail of the

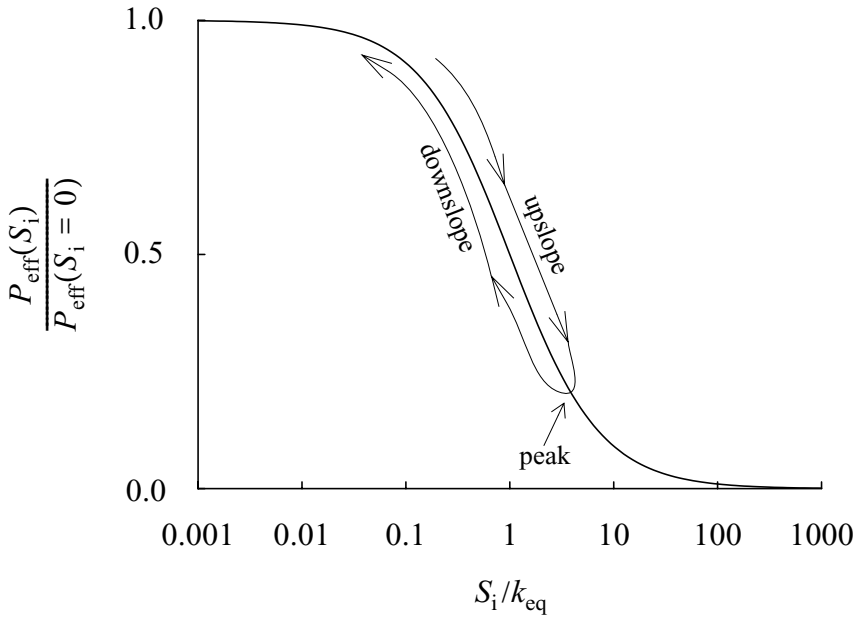

Figure 8-15: The idea of the "bolus sweep" indicator dilution experiment. Tracer and non-tracer "mother" solute are injected together into the inflow to an organ in a multiple indicator dilution experiment and the outflow concentration time-curve is obtained. Mother substance competes with tracer for the binding site on the transporter in accord with its concentration; tracer concentrations are by definition negligible. The peak competition occurs at the peak of the dilution curve. (See Figure 8-16.)

washout. Note that the initial point of $E(t)$ is less than this maximum, indicating that there was some inhibition to tracer transport by the non-tracer concentration in the first sample. The non-tracer concentration is not plotted: while if extraction were low it would have a shape close to that of the reference tracer dextran, in this case with high tracer extraction, there will also be extraction of non-tracer, about 20% at the peak concentration.

Serotonin (also known as 5-HT or hydroxytryptamine), like PGE_1, is taken up by endothelial cells and rapidly converted to a product which doesn't leave the cell (5-HT $\rightarrow$ 5-HIAA, or, in words, 5-hydroxytryptamine $\rightarrow$ 5-hydroxyindole acetic acid). There is, however, some small return flux of serotonin which reduces $E(t)$ during the tail. (Why is the reduction in $E(t)$ more for the 10 nmol dose than for the 100 nmol dose?)

The bolus sweep experiment has one great advantage over performing a set of several indicator dilution curves at different background non-tracer levels: the total mass of the solute injected in the bolus is very much less than is administered during steady infusions and the experiment is over before any physiological responses occur.

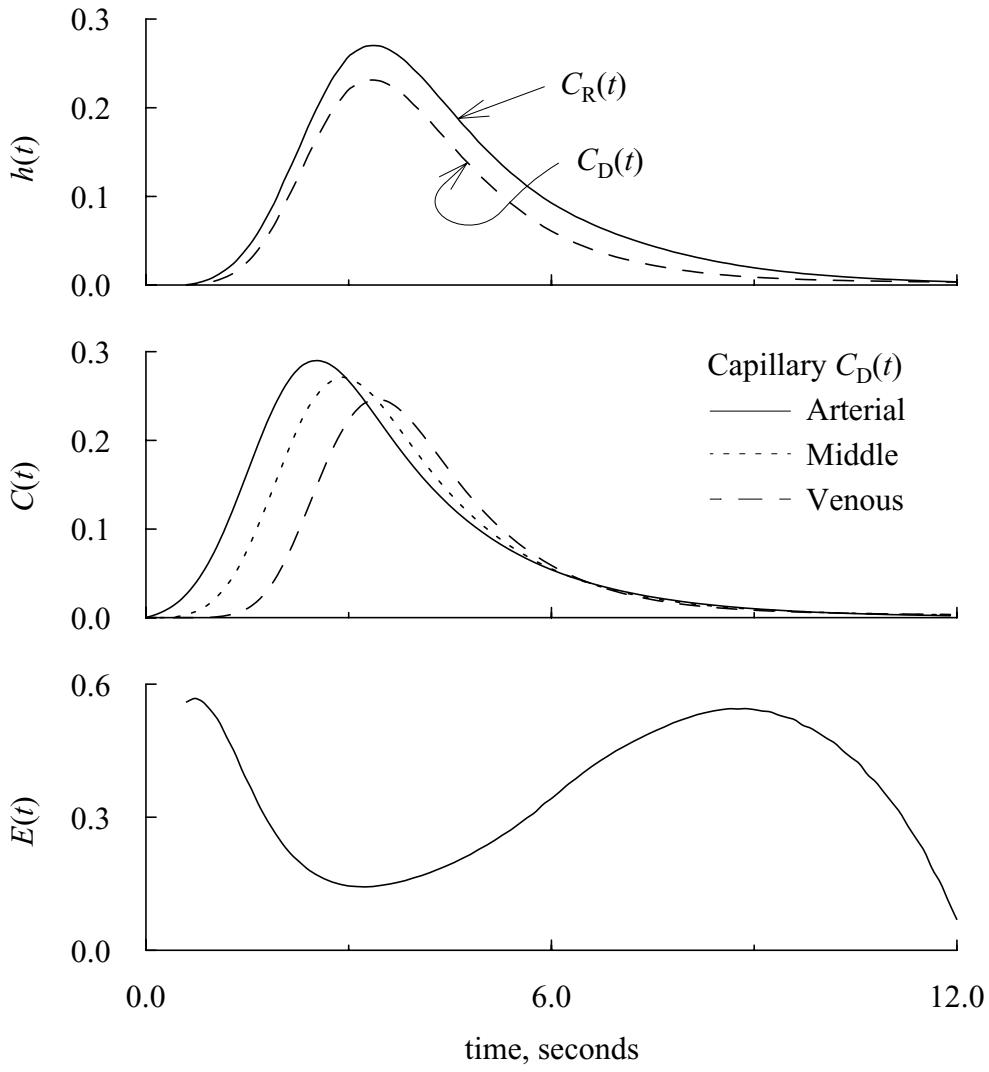

Figure 8-16: Tracer transients using the "bolus sweep" method for a solute transported across the luminal endothelial surface and consumed entirely within the endothelial cell. *Upper:* Outflow $C_R(t)$ and $C_D(t)$ normalized. *Middle:* Concentration-time curves within the capillary at upstream, midstream and downstream positions. *Lower:* The P_{eff} was reduced to about one-quarter of its zero-competition value by the peak concentration of non-tracer mother solute in the bolus, as shown by the nadir in $E(t)$. Parameters were **??**

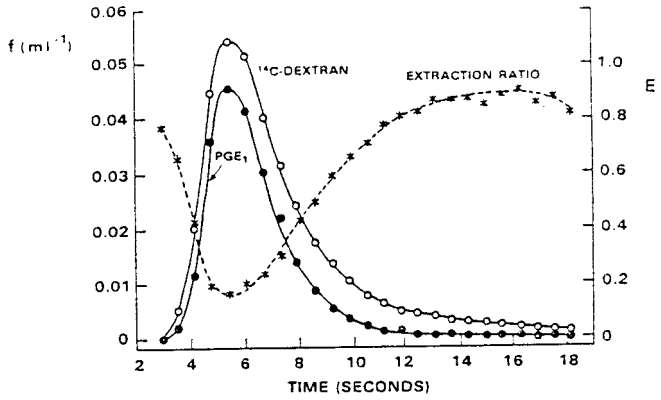

Figure 8-17: Prostaglandin E_1, tracer outflow dilution curve from the lung. The bolus contained a near saturating dose of PGE_1. The instantaneous extraction, $E(t)$, returns to 90% during the washout phase. From Linehan et al. [1981] with permission)

8-5. Energetically coupled transporters: Ion pumps

8-5.1. General features: Energy transduction, influence of membrane potential, influence on the action potential

8-5.2. The Sodium Pump, the NaK ATPase

8-5.3. The Calcium Pump, the Ca ATPase

8-5.4. The Sodium-Calcium Exchanger (secondary energetic coupling)

8-6. Coupled ionic fluxes, charge-neutral exchangers

8-6.1. Sodium-Hydrogen exchanger

8-6.2. Electroneutral co-tranpsporters

8-7. Problems

1. In steady-state experiments on fluxes between two stirred tanks separated by a membrane, draw a graph and write an equation describing the effect of increasing the steady-state concentration in the source chamber with no solute in the sink chamber.
2. Compare and contrast the Barrer time-lag method for estimating the rate of diffusion through a membrane with the initial velocity method of this chapter. Consider the membrane, the transporters, binding sites, etc.
3. When there is no transporter, how would the earliest concentrations in the recipient chamber in an initial velocity experiment using a thick membrane differ from those using a thin membrane? With binding sites in the membrane? With a transporter?
4. Show the reduction of the equations for a transporter to the simple Michaelis-Menten expression for saturable transport.
5. Based on the model code for the simple transporter, write the expression for the unidirectional flux of substrate from side 2 to side 1.
6. Using the model for a transporter with a single binding site, define the conditions under which the unidirectional flux of A from V1 to V2 would be enhanced by the presence of A on side 2 (A2 > 0).
7. Start with Code **facT1.proj** and load parfameter set **facT1.satn3.par**: **PLOTPAGE 3**:
   Use CVODE as the solver. Run for 1e4 seconds at dt = 0.25sec.
   The conditions set up here are that A1(0) = 100*Kd for binding and A2(0) = 0.
   The transport rate is low, but V2 is small so that the concentration A2 builds up faster than A1 is depleted.
   V1*dA1/dt = flux out of V1.= red curve
   V2*dA2/dt = flux into V2. = green curve
   A2 rises from well below Kd to 60 times Kd at 10000 seconds.
   Explain:
   (1) What events cause the red and the green curves to differ.

(2) Why do they converge?
(3) Why does V2*dA2/dt have a minimum at early times and then become constant for a while.
(4) What will be the final values of the two fluxes at t = infinity?
(5) V1*dA1/dt = constant from 1 to 40 seconds. How is this compatible with the changing flux, V2*dA2/dt?

8. Design a counter transport facilitation/inhibition experiment to see if $P' \neq 1$. (We will learn in later chapters that a convection-diffusion-permeation-reaction model, Gentex, can be used for this in representing [to represent -ed.] blood–tissue exchange *in vivo*.)
9. Describe and explain the conditions under which a single-site transporter which can bind either of two similar substrates competitively, A or B, can demonstrate the following behavior: Volumes on side 1 and side 2 are equal. Ignore the possibility of osmotic water flux. Solute A is initially 10 mM on side 1, zero on side 2; A1diminishes to less than 4 mM on side 1 and A2 rises to above 6 mM on side 2, and thereafter both A1 and A2 gradually approach a concentration just below 5 mM. The solute B is available.
10. What are the determinants of the maximal countertransport facilitation? Can you develop an approximate expression for this?
11. Fig. 8-14 illustrates that substrate on the opposite side of the membrane can increase the apparent permeability. What is the effective permeability in the program in Table 1? Using the parameters in the Table 1 code, calculate $P_{eff}/(0.5\ T_T\ P_{TS})$ for an infinitely high concentration on the opposite side.

8-8. References

Agre P, Preston GM, Smith BL, Jung JS, Raina S, Moon C, Guggino WB, and Nielsen S. Aquaporin CHIP: the archetypal molecular water channel. Am J Physiol Renal Physiol 265: F463-F476, 1993.

Crone C. Facilitated transfer of glucose from blood into brain tissue. *J Physiol* 181: 103-113, 1965.

Dawson CA, Linehan JH, Rickaby DA, and Roerig DL. Influence of plasma protein on the inhibitory effects of indocyanine green and bromcresol green on pulmonary prostaglandin E_1 extraction. *Br J Pharmac* 81: 449-455, 1984.

Foster DM and Jacquez JA. An analysis of the adequacy of the asymmetric carrier model for sugar transport. *Biochim Biophys Acta* 436: 210-221, 1976.

Klingenberg M. Membrane protein oligomeric structure and transport function. *Nature* 290: 449-454, 1981.

Linehan JH, Dawson CA, and Wagner-Weber VM. Prostaglandin E_1 uptake by isolated cat lungs perfused with physiological salt solution. *J Appl Physiol 50:* 428-434, 1981.

Linehan JH, Bronikowski TA, and Dawson CA. Kinetics of uptake and metabolism by endothelial cell from indicator dilution data. *Ann Biomed Eng* 15: 201-215, 1987.

Plagemann PGW and Wohlhueter RM. Permeation of nucleosides, nucleic acid bases, and nucleotides in animal cells. *Curr Top Membr Transp* 14: 225-330, 1980.

Rickaby DA, Linehan JH, Bronikowski TA, and Dawson CA. Kinetics of serotonin uptake in the dog lung. *J Appl Physiol 51 (Respirat. Environ. Exercise Physiol* 2): 405-414, 1981.

Schwartz LM, Bukowski TR, Ploger JD, and Bassingthwaighte JB. Endothelial adenosine transporter characterization in perfused guinea pig hearts. *Am J Physiol Heart Circ Physiol* 279: H1502-H1511, 2000.

Stein WD. *The Movement of Molecules across Cell Membranes.* New York: Academic Press, 1967.

Stein WD. *Transport and Diffusion across Cell Membranes.* Orlando, Florida: Academic Press Inc., 1986.

Tanford C. *Physical Chemistry of Macromolecules.* New York: John Wiley & Sons, 1961.

ter Kuile BH and Westerhoff HV. Transcriptome meets metabolome: hierarchical and metabolic regulation of the glycolytic pathway. *FEBS Lett* 500: 169-171, 2001.

Wilbrandt W and Rosenberg T. The concept of carrier transport and its corollaries in pharmacology. *Pharmacol Rev* 13: 109-183, 1961.

Winslow RL, Rice J, Jafri S, Marbán E, and O'Rourke B. Mechanisms of altered excitation-contraction coupling in canine tachycardia-induced heart failure, II: Model studies. *Circ Res* 84: 571-586, 1999.

NOTES:

Cases for $P' \neq 1$ are considered next.

Convert Fg 8-5 the code for TranspMM to a table

Find figure for 8-9